

UC San Diego

UC San Diego Previously Published Works

Title

Dendrimeric Guanidinoneomycin for Cellular Delivery of Bio-macromolecules

Permalink

<https://escholarship.org/uc/item/70d9x6v1>

Journal

ChemBioChem, 18(1)

ISSN

1439-4227

Authors

Sganappa, Aurora
Wexselblatt, Ezequiel
Bellucci, Maria Cristina
[et al.](#)

Publication Date

2017-01-03

DOI

10.1002/cbic.201600422

Peer reviewed



Dendrimeric Guanidinoneomycin for Cellular Delivery of Bio-macromolecules

Aurora Sganappa^{+, [a]}, Ezequiel Wexselblatt^{+, [b]}, Maria Cristina Bellucci,^[c] Jeffrey D. Esko,^[d] Gabriella Tedeschi,^[e] Yitzhak Tor,^{*[b]} and Alessandro Volonterio^{*[a]}

This paper is dedicated to the memory of Prof. Pierfrancesco Bravo

We present the synthesis of polymeric amino- and guanidinoglycosides prepared by tethering neomycin and guanidinoneomycin to PAMAM dendrimers of generations 2 and 4. The ability of these conjugates to promote cellular uptake of high-molecular-weight cargo is discussed, together with their cytotoxicity and mechanisms of entry. We demonstrate that the pres-

ence of multiple guanidinoneomycin carriers on the PAMAM surface plays an important role in promoting cellular uptake of the dendrimers, maintaining the heparan sulfate specificity and negligible cytotoxicity typical of monomeric guanidinoglycoside molecular transporters.

Introduction

The interest in developing new guanidinium-rich molecular transporters increased dramatically over the past 20 years, after the ability of HIV-1 Tat to cross cell membranes was recognized and attributed to the presence of guanidinium groups.^[1,2] Indeed, such agents have previously been shown to facilitate the cellular internalization of diverse high-molecular-weight (high-MW) biologicals, such as peptides, proteins, and enzymes, as well as of low-MW drugs that are precluded from clinical use because of their inability to cross cell membranes. Consequently, different cell-penetrating peptides (CPPs) and CPP-like oligomers—including polyarginines,^[3] polyprolines,^[4] poly- β -peptides,^[5] peptoids,^[6] oligocarbamates,^[7] guanidinylated PNAs,^[8] and very recently oligophosphoesters^[9]—have been

developed over the years. The disadvantages of certain CPPs originate from nonspecificity, susceptibility to proteolytic degradation, and expensive scale-up production.^[10] Therefore, the development of new guanidinium-rich molecular transporters that could potentially overcome these limitations is desirable.

From a chemical point of view, the construction of multi-guanidinylated molecules/polymers requires so-called “guanidylating agents”, which promote the transformation of amino groups into guanidine moieties in a very efficient and selective way.^[11] Indeed, direct guanidinylation of natural aminoglycoside antibiotics afforded guanidinoglycosides, a class of guanidinium-rich efficient molecular transporters.^[12] These delivery vehicles are intriguing for several reasons, the most powerful being: 1) unlike other guanidinium-rich transporters, their cellular delivery occurs at nanomolar concentrations, 2) their uptake exclusively depends on the presence of heparan sulfate proteoglycans (HSPGs), 3) they have been shown to induce HPSG aggregation, which is an important step for endocytic entry, and 4) their efficiency depends on the valency of the carriers.^[13] The last point prompted us to investigate cooperativity in the cellular uptake of multimeric guanidinoglycosides conjugates. Here we report the synthesis and characterization of polyamidoamine PAMAM-guanidinoneomycin (PAMAM-GNeo) conjugates of two different generations (G2 and G4) obtained by anchoring GNeo to the outer free amino groups of the dendrimer through a suitable linker.

PAMAM dendrimers have been utilized for noncovalent encapsulation of different drugs for the facilitation of aqueous solubility and cellular uptake.^[14] Being peptide mimics, and thus biocompatible for drug delivery applications, PAMAM dendrimers are a significant alternative to CPPs, due to their cost-effective preparation on a multigram scale with a high level of control over the dendritic architecture (size, branching density, surface functionality), along with the so-called “enhanced penetration and retention (EPR)”.^[15] Dendrimers can

[a] Dr. A. Sganappa,⁺ Prof. Dr. A. Volonterio
Department of Chemistry
Material and Chemical Engineering “Giulio Natta”
Politecnico di Milano
via Mancinelli 7, 20131 Milano (Italy)
E-mail: alessandro.volonterio@polimi.it


[b] Dr. E. Wexselblatt,⁺ Prof. Dr. Y. Tor
Department of Chemistry and Biochemistry, University of California
9500 Gilman Drive, La Jolla, CA 92093 (USA)
E-mail: ytor@ucsd.edu

[c] Dr. M. C. Bellucci
Department of Food, Environmental and Nutritional Sciences
Università degli Studi di Milano
Via Celoria 2, 20133 Milano (Italy)

[d] Prof. Dr. J. D. Esko
Department of Cellular and Molecular Medicine, University of California
9500 Gilman Drive, La Jolla, CA 92093 (USA)

[e] Prof. Dr. G. Tedeschi
Department of Veterinary Science and Public Health
Università degli Studi di Milano
Via Celoria 2, 20133 Milano (Italy)

[*] These authors contributed equally to this work.

 Supporting information and the ORCID identification numbers for the authors of this article can be found under <http://dx.doi.org/10.1002/cbic.201600422>.

also be developed to be resistant to biodegradation, and, most importantly, they can be easily functionalized at the outer amines.^[16] For these reasons, PAMAM and related polyamide dendrimers have been functionalized with guanidinium-containing moieties for exploring cellular internalization. In this work we demonstrate that multivalent PAMAM-GNeo conjugates can efficiently promote cellular uptake of a large bioactive molecule through biotin–streptavidin interactions with little or no cellular cytotoxicity, opening up the possibility of using them as general drug delivery vehicles.^[16]

Results and Discussion

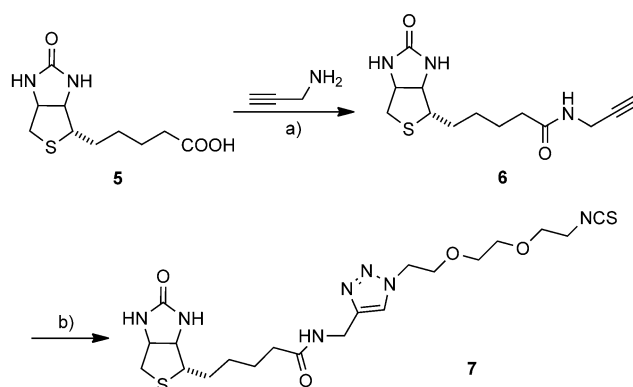
Synthesis and characterization of biotin-PAMAM-(G)Neo conjugates

Two different generations of PAMAM dendrimers—generation two (PAMAM G2) and generation four (PAMAM G4)—were decorated with GNeo moieties. The synthetic strategy used is based on the reaction between isothiocyanate-modified GNeo and PAMAM dendrimers, resulting in the clean formation of stable thiourea conjugates as previously exploited.^[17] Accordingly, GNeo-isothiocyanate **4** was synthesized through an azide–alkyne “click” reaction between GNeo derivative **2**^[13] and hetero-bifunctionalized oligo(ethylene glycol) linker **3**, prepared as reported in the Supporting Information (Schemes 1 and S1).

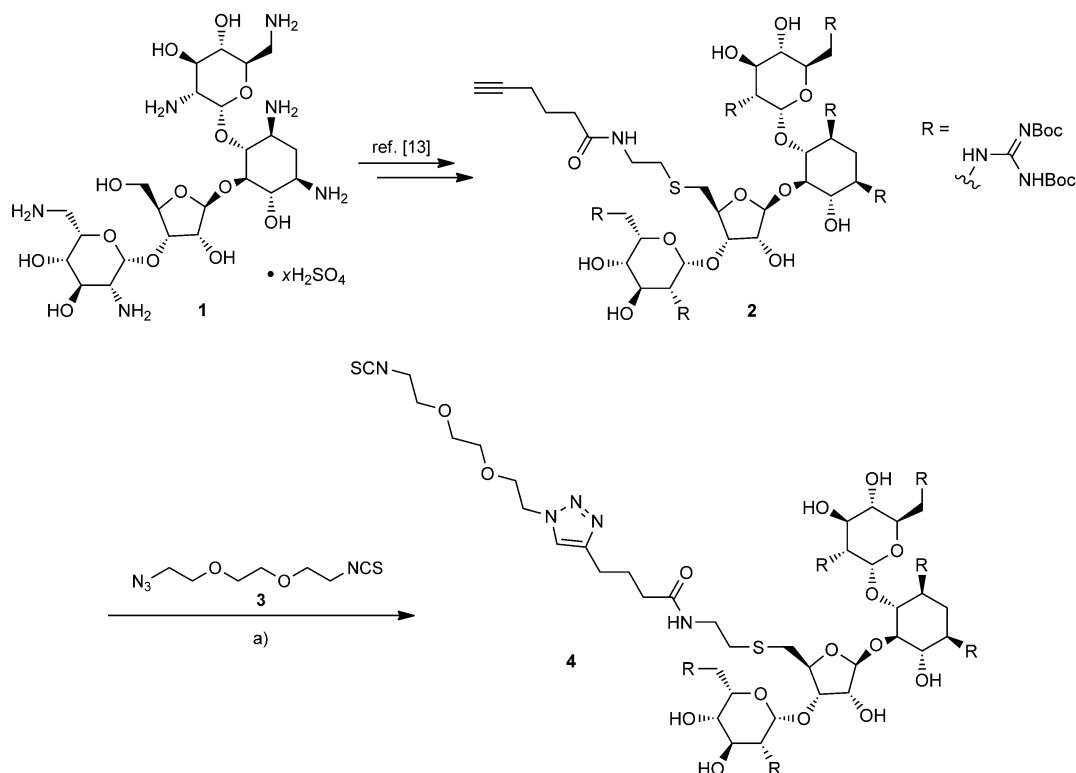
To assess the ability of PAMAM-GNeo carriers to deliver high-molecular-weight cargo into cells we used fluorescent strepta-

vidin-phycoerythrin-Cy5 (ST-PECy5, MW 300 kD) as a model payload. Because streptavidin forms a very stable tetrameric complex with biotin, a biotin-isothiocyanate derivative was synthesized by anchoring biotin to the same linker as used for GNeo. Thus, biotin (**5**) was coupled to propargylamine through EDC (*N*-(3-dimethylaminopropyl)-*N*-ethylcarbodiimide) chemistry to produce intermediate **6**, which was clicked with hetero-bifunctionalized linker **3** to afford biotin-isothiocyanate **7** (Scheme 2).

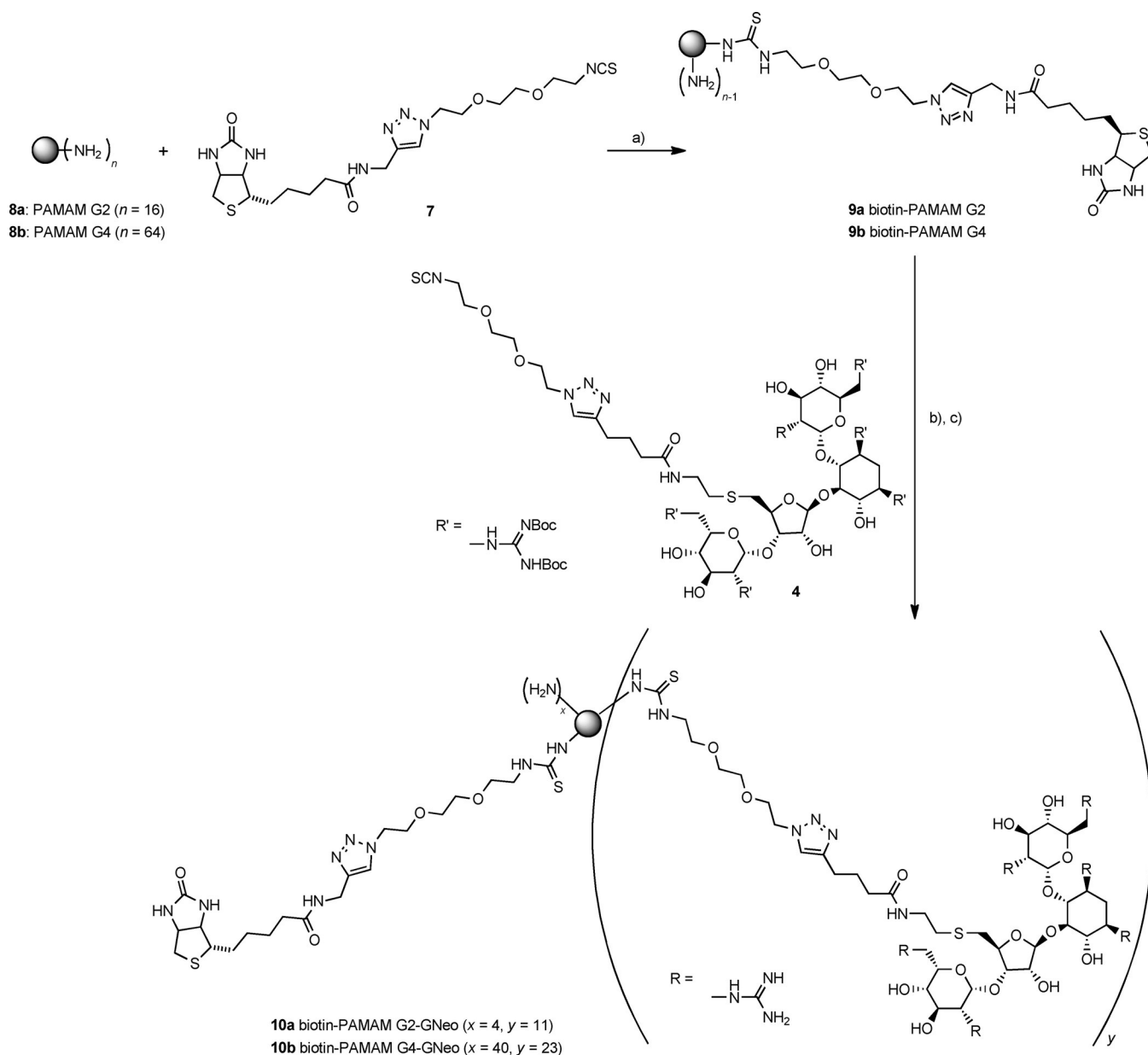
Isothiocyanate–amine click reactions between one equivalent of biotin-isothiocyanate **7** and commercially available PAMAM G2 (**8a**) and PAMAM G4 (**8b**) were performed in DMSO at 40 °C over 12 h., leading to the formation of biotin-



Scheme 2. Synthesis of biotin-isothiocyanate **7**. a) EDC, DIPEA, CH₂Cl₂ (94%); b) **3**, Cu(OAc)₂, Na ascorbate, MeOH/THF/H₂O (68%).



Scheme 1. Synthesis of GNeo-isothiocyanate **4**. a) Cu(OAc)₂, Na ascorbate, MeOH/THF/H₂O (81%).



Scheme 3. Synthesis of biotin-PAMAM-GNeo conjugates **10a** and **10b**. a) DMSO, 40 °C, 12 h; b) DMSO, 40 °C, 24 h; c) TFA.

PAMAM conjugates **9a** and **9b**, respectively (Scheme 3). The presence of the biotin linker in the final dendrimers was confirmed by ^1H NMR spectroscopic examination of the final conjugates, in which the signals corresponding to the biotin heterocycle and to the linker were identified (see stacked spectra in the Supporting Information). Finally, biotin-PAMAM conjugates **9a** and **9b** were treated with GNeo-isothiocyanate **4** under the same conditions—DMSO at 40 °C for 24 h—with use of an excess of 1.1 equivalents per free primary dendrimeric amine to maximize the degree of grafting, producing, after final deprotection with trifluoroacetic acid (TFA), biotin-PAMAM G2-GNeo (**10a**) and biotin-PAMAM G4-GNeo (**10b**), containing 11 and 23 GNeo moieties, respectively (Scheme 3).

To determine the effect of GNeo on cellular uptake we also prepared the corresponding biotinylated PAMAM G2-Neo (**11a**)

and PAMAM G4-Neo (**11b**), bearing ten and 32 neomycin residues, respectively, by the same synthetic strategy (Scheme S2). The higher degree of grafting observed for PAMAM G4-Neo is most likely due to Neo being less sterically hindered than GNeo. The degrees of grafting of all the dendrimer conjugates were initially calculated by integration of the characteristic ^1H NMR signals of Neo and GNeo derivatives. The three singlets corresponding to the protons linked to the anomeric carbons (which resonate between 5 and 6 ppm), the triazole proton (resonating around 8 ppm), and the methylene protons belonging to the 2-deoxystreptamine ring (resonating around 2.1 and 1.6 ppm, respectively), were compared with the multiplet resonating between 2.6 and 3.0 ppm, corresponding to the methylene protons in the α position to the carbonyl group in the PAMAM dendrimers (248 for PAMAM G4 and 56 for

PAMAM G2) and with the six methylene protons in the α position to the carbonyl group and the sulfur atom in the Neo and GNeo moieties (see ^1H and $^1\text{H},^1\text{H}$ COSY NMR in the Supporting Information). The calculated degrees of grafting were further supported by MALDI spectroscopy, through which the average molecular masses of the dendrimers were measured and compared with the calculated ones. Table 1 lists the mass spectrometry data.

Table 1. Molecular masses determined by MALDI mass analysis and the corresponding values calculated for the single charged parent ions.

Dendrimer	<i>m/z</i> value	
	Experimentally measured	Calculated $[M+H]^+$
1 PAMAM G2 (9a)	3256	3256
2 biotin-PAMAM G2-Neo (11a)	13663	13593
3 biotin-PAMAM G2-GNeo (10a)	17361	17349
4 PAMAM G4 (9b)	13266	14215
5 biotin-PAMAM G4-Neo (11b)	45158	45738
6 biotin-PAMAM G4-GNeo (10b)	41621	42191

Cellular uptake of PAMAM-(G)Neo conjugates

To evaluate the ability of the decorated dendrimers to deliver high-molecular-weight bio-macromolecules to cells, fluorescently labeled streptavidin-phycoerythrin (ST-PECy5, 300 kDa) was complexed to the biotin handle in the carriers. Uptake was evaluated in wild-type Chinese hamster ovary (CHO-K1) cells. The cells were incubated with the complexes (2 nM) at 37 °C for 1 h and analyzed by flow cytometry. The mean fluorescence intensities (MFIs) of the cells treated with PAMAM G4 complexes **10b** and **11b** are significantly higher than those of the signals arising from cells treated with their PAMAM G2 counterparts **10a** and **11a** (Figure 1A). Moreover, the signals obtained with the GNeo derivatives **10a** and **10b** are stronger than those obtained with the corresponding neomycin derivatives **11a** and **11b**. Furthermore, for both PAMAM G2 and PAMAM G4 the signal obtained for the undecorated carrier—**9a** and **9b**, respectively—was the lowest (Figure 1A). As expected, these data demonstrated that the multivalent presence of either Neo or GNeo moieties on the PAMAM's perimeter increases the cellular uptake of the dendrimers, with GNeo-decorated dendrimers being much more efficient than Neo-decorated dendrimers.

Further, to quantify the effect of multivalency on cellular uptake and to assess the contribution of either Neo or GNeo moieties to the enhanced cellular uptake, the MFI values were normalized to the number of moieties and compared with those for monomeric biotinylated Neo and GNeo (for the synthesis, see the Supporting Information). Consistently with our previously reported observations,^[12b] monomeric GNeo displayed higher cellular uptake than monomeric Neo (Figure 1B). Relative to the monomeric neomycin, the dendrimeric Neo derivatives show a 15- and a ninefold increase per moiety for PAMAM G4 and PAMAM G2, respectively (detailed in Table S1). Relative to the monomeric GNeo, there is a 1.7-fold increase

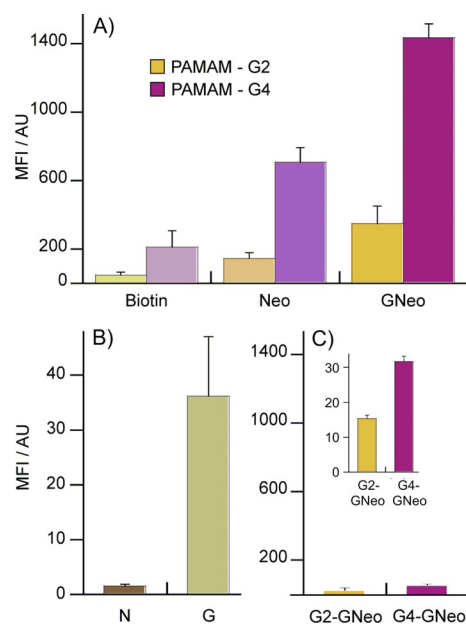


Figure 1. Cellular uptake. Cells were incubated with dendrimeric carriers complexed to fluorescently labeled streptavidin (ST-PECy5) for 1 h at 37 °C. MFI was measured by flow cytometry. The background signal from untreated cells was subtracted. A) Wild-type CHO-K1 cells incubated with ST-PECy5 (2 nM) complexed to undecorated polyamidoamine G2 or G4 (biotin) or to PAMAM decorated with either neomycin (Neo) or guanidinoneomycin (GNeo) as indicated. B) Wild-type CHO-K1 cells incubated with ST-PECy5 (2 nM) complexed to “monomeric” neomycin (N) or guanidinoneomycin (G). C) Mutant pgsA-745 cells incubated with GNeo-decorated PAMAM G2 or PAMAM G4, as indicated. Error bars each represent the standard deviation from an average of three experiments, each of them at least in triplicate.

for PAMAM G4. However, for PAMAM G2 the contribution of each GNeo moiety to the MFI is similar to that of its “monomeric” form. Indeed, for PAMAM systems decorated with Neo, which by itself is not able to promote cellular uptake in an efficient way, there is an important increase in efficiency per moiety of aminoglycoside; this probably reflects the presence of more cationic moieties, which promote a tighter interaction with negatively charged cell-surface residues (this is also demonstrated by the best efficiency in promoting cellular uptake of PAMAM systems decorated with Neo moieties relative to undecorated PAMAM dendrimers). This effect is negligible for GNeo-decorated PAMAM systems, in which the binding of the guanidine moieties of the GNeo moieties with HSPGs is already very strong and selective.

Indeed, we have previously reported that cellular uptake of guanidinoneomycin-based carriers is highly dependent on the presence of glycosaminoglycans (GAGs) on the cell surfaces.^[12] To demonstrate that this selectivity is maintained for the dendrimeric guanidinoneomycin carriers, their cellular uptake was tested in a mutant pgsA-745 cell line that lacks heparan sulfate and chondroitin/dermatan sulfate.^[18] Highly reduced cellular uptake was observed for both PAMAM G2 and PAMAM G4 decorated with guanidinoneomycin, indicating a high selectivity of these dendrimers for cell surface GAGs.

Finally, we investigated the cytotoxicity of PAMAM-GNeo and PAMAM-Neo conjugates **10a**, **10b**, **11a**, and **11b** by means of a Cell Titer Blue assay. Interestingly, all the dendrim-

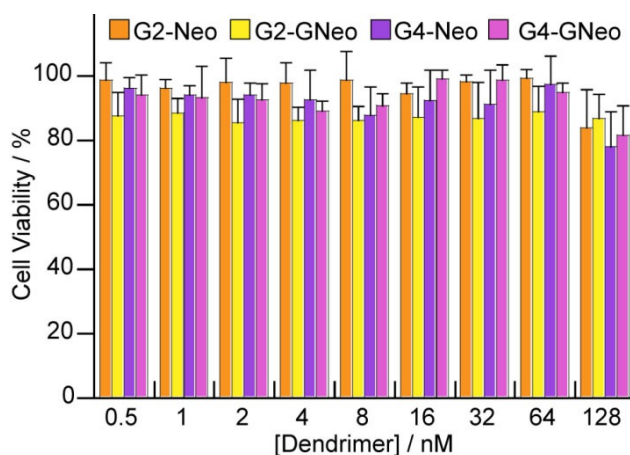


Figure 2. Cytotoxicity profile of PAMAM-(G)Neo dendrimers.

ers were found to be nontoxic at concentrations up to about 15 times higher than those used in cellular uptake experiments (Figure 2).

Mechanisms of uptake

To better understand the internalization mechanisms of these carriers, the contributions of different endocytotic pathways were evaluated. Cellular uptake was tested at low temperature (to assess the involvement of energy-dependent processes) and in cells pretreated with sucrose (preventing clathrin-mediated endocytosis) or with amiloride (perturbing macropinocytosis). Interestingly, at low temperatures the cellular uptake of PAMAM G2-GNeo is reduced to about 35% whereas the other complexes display only between 5 and 10% of internalization relative to that seen at 37 °C (Figure 2A and B). Notably, internalization of neomycin-decorated dendrimers was almost fully prevented by pretreating the cells either with sucrose or with amiloride. Furthermore, in cells pretreated with sucrose, the cellular uptake of undecorated dendrimers was reduced to about 50 and 70%, and in cells pretreated with amiloride the internalization decreased to about 20 and 30% for PAMAM G2 and PAMAM G4, respectively. Unlike the effect seen for GNeo-protein conjugates^[12b] and for GNeosomes,^[19] the entry of GNeo-decorated dendrimers is only lowered to about 60 and 50% in cells pretreated with sucrose and to about 50 and 70% in cells pretreated with amiloride for PAMAM G2 and PAMAM G4, respectively.

Taken together, these results suggest that energy-dependent pathways are involved in the internalization of PAMAM G2 carriers to a greater extent than for their PAMAM G4 counterparts. Interestingly, the mechanisms of entry of PAMAM dendrimers decorated with Neo and GNeo moieties seem to be different. In particular, the behavior of the GNeo polymers appears to be mainly influenced by the presence of the PAMAM moiety. Whereas monomeric GNeo is likely internalized through clathrin-dependent endocytosis,^[12b] cells pretreated with sucrose do not show any marked decrease in internalization either of PAMAMs or of PAMAM-GNeos; treatment with amiloride has

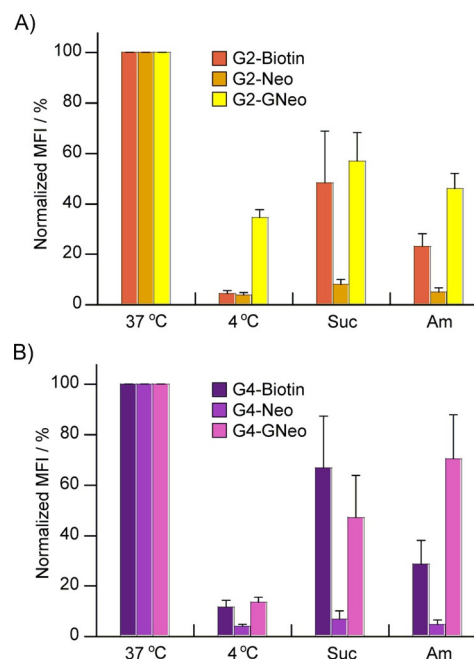


Figure 3. Mechanisms of uptake. CHO-K1 cells were incubated with ST-PECy5 (2 nm) complexed to undecorated biotin-PAMAM G2 or G4 or to biotin-PAMAM decorated with either Neo or GNeo as indicated. Cellular uptake was evaluated at 37 and at 4 °C. Cells were treated with sucrose (Suc, 1 h, 400 mM) or amiloride (Am, 10 min, 5 mM) at 37 °C prior to incubation with the complexes. MFIs were measured by flow cytometry. The background signals from untreated cells were subtracted, and the MFIs were normalized. A) PAMAM G2. B) PAMAM G4.

an observable effect, even if not as marked as for PAMAM dendrimers (Figure 3).

Conclusion

To summarize, we have synthesized GNeo-decorated PAMAM dendrimers of two different generations and compared their performances as molecular transporters of high-molecular-weight cargos with those of the corresponding PAMAM-Neo oligomers and undecorated PAMAM dendrimers. The results provided clear evidence for the importance of multivalent GNeo presentation on the dendrimer periphery for achieving efficient uptake. Interestingly, PAMAM decorated with Neo moieties also showed better propensity to cross the cell membrane than the undecorated dendrimers, despite monomeric neomycin being inefficient. The effect of multivalency on cellular uptake was assessed by comparison with the behavior of monomeric GNeo and Neo. Whereas there is a substantial increase in efficiency for the PAMAM-Neo conjugates, probably due to the presence of more cationic moieties, this effect is negligible for PAMAM systems decorated with GNeo moieties. This result, along with the highly reduced cellular uptake in cells lacking GAGs, again demonstrated the importance and the strength of the binding between GNeo and HSPGs. Importantly, such oligomers appear to be nontoxic at concentrations up to about 15 times higher than those needed for effective cellular uptake. All these results suggest that PAMAM-GNeo

oligomers could be used as general efficient vehicles for drug delivery.

Experimental Section

Materials: Neomycin sulfate, PAMAM G4 dendrimer (ethylenediamine core, 64 surface groups), PAMAM G2 dendrimer (ethylenediamine core, 16 surface groups), and all other organic reactants, solvents, and culture reagents were purchased from Sigma–Aldrich if not differently specified and were used as received. Spectra/Por dialysis bags (MWCO = 1 and 8 kDa) were from Spectrum Laboratories (Compton, CA, USA). Dulbecco's phosphate-buffered saline (PBS), F-12 Nutrient Mixture (Ham), Dulbecco's modified Eagle's medium (DMEM), fetal bovine serum (FBS), and streptavidin-PECy5 were purchased from Life Technologies. Trypsin/EDTA was purchased from VWR (Mediatech, Manassas, VA, USA). Costar 3524 (Corning) 24-well plates were used. ^1H NMR spectra were recorded with 400 and 500 MHz spectrometers. Chemical shifts are expressed in ppm (δ) with tetramethylsilane (TMS) as internal standard for ^1H and ^{13}C nuclei (δ_{H} and $\delta_{\text{C}} = 0.00$). MALDI-TOF analysis was carried out with a Bruker Daltonics Reflex IV instrument equipped with a nitrogen laser (337 nm) and operated in linear mode with use of the dry droplet technique and 2,3-dihydroxybenzoic acid (10 mg mL^{-1}) in $\text{CH}_3\text{CN}/\text{TFA}$ (1:1) as a matrix. External standards were used for calibration (Bruker protein calibration standards 1 and 2). Each spectrum was accumulated for at least 600 laser shots. Mass spectra were recorded at the UCSD Chemistry and Biochemistry Mass Spectrometry Facility; low-resolution mass spectrometry (LRMS) analysis was performed with a Thermo LCQdeca mass spectrometer and use of electrospray ionization (ESI) as the ion source. An Agilent 6230 time-of-flight mass spectrometer (TOF-MS) was employed for HRMS analysis with use of ESI as the ion source. Reversed-phase HPLC purification (CLIQUEUS, C_{18} , $5\ \mu\text{m}$, $10 \times 250\ \text{mm}$, Higgins Analytical) and analysis (Eclipse, XDB- C_{18} , $5\ \mu\text{m}$, $4.6 \times 150\ \text{mm}$) were carried out with an Agilent 1200 series instrument. Flow-cytometry studies were performed with a BD FACSCalibur.

Decoration of biotin-PAMAM dendrimers with (G)Neo—General Procedure: The biotin-decorated PAMAM G2 and PAMAM G4 were dissolved in DMSO (1 mL per 10 mg of the dendrimer). A solution of Neo-isothiocyanate **16** or GNeo-isothiocyanate **4** (1.1 equiv per NH_2 group) in a minimum amount of DMSO was added, and the solution was stirred at 40°C for 24 h. The solution was dialyzed (MW cutoff 8 kDa) against MeOH (10 h, the solvent reservoir was renewed three times). The organic solvent was evaporated, and the resulting decorated dendrimers were treated with neat TFA (1 mL) for 30 min. The TFA was evaporated under reduced pressure and co-evaporated three times with toluene to afford the final biotin-PAMAM-(G)Neo conjugates.

Cell culture: All cells were grown under CO_2 (5%) in air and at 100% relative humidity. Wild-type CHO-K1 cells were obtained from the American Type Culture Collection (CCL-61), and pgsA-745 cells were prepared as previously reported.^[18] CHO-K1 and pgsA-745 cells were grown in F-12 medium supplemented with FBS (10%, v/v), streptomycin sulfate ($100\ \mu\text{g mL}^{-1}$), and penicillin G ($100\ \text{units mL}^{-1}$).

Cellular uptake: In a typical experiment, biotinylated dendrimer ($7.5\ \mu\text{M}$) was incubated with ST-PECy5 ($1.5\ \mu\text{M}$) for 20 min at ambient temperature and then diluted with cell culture medium to yield conjugate solutions at final ST-PECy5 concentrations of 2 nM. Wild-type CHO-K1 and mutant pgsA-745 cells were seeded onto

24-well tissue culture plates (100 000 cells per well, 0.5 mL) and grown for 24 h to about 80% confluence. Cells were washed with PBS and incubated with the streptavidin–dendrimer complexes ($300\ \mu\text{L}$), diluted in DMEM to 2 nM, and incubated at 37°C for 1 h under CO_2 (5%). The cells were washed twice with PBS ($500\ \mu\text{L}$), detached with trypsin/EDTA ($100\ \mu\text{L}$) at 37°C for 5 min, diluted with PBS containing BSA (1%, $300\ \mu\text{L}$), and analyzed by FACS.

Evaluation of clathrin-dependent endocytosis and macropinocytosis of decorated PAMAM dendrimers: Cells were grown for 24 h as described above, washed with PBS, and incubated with sucrose (400 mM) or amiloride (5 mM) for 1 h or 10 min, respectively. Cells were then washed with PBS, treated with the carrier-streptavidin complexes diluted in DMEM (2 nM, $300\ \mu\text{L}$), and further incubated at 37°C for 1 h under CO_2 (5%). Cells were washed with PBS, detached with trypsin/EDTA, and analyzed as described above.

Evaluation of uptake dependency on temperature: Cells were grown for 24 h as described above, washed with PBS, and incubated for 30 min at 4°C in DMEM. Pre-cooled carrier-streptavidin complexes, diluted in DMEM to 2 nM, were added to the cooled cells and incubated for 30 min at 4°C . Cells were washed, detached, and analyzed as described above.

Cell viability: CHO-K1 cells were seeded in a 96-well plate at a density of 20 000 cells per well ($200\ \mu\text{L}$). After growing overnight, the cells were washed and treated with dendrimeric neomycin or guanidinoneomycin diluted to the indicated concentrations in DMEM and incubated for 24 h at 37°C under CO_2 (5%). Cells were then washed, and the growth medium was replaced by fresh ($100\ \mu\text{L}$). CellTiter-Blue ($20\ \mu\text{L}$) was added to each well, and the cells were incubated for 4 h at 37°C . Fluorescence was measured in a plate reader with $\lambda_{\text{ex}} = 530\ \text{nm}$, $\lambda_{\text{em}} = 580\ \text{nm}$. Fluorescence intensity was normalized to that of untreated cells.

Acknowledgements

This work was partially supported by the Politecnico di Milano. We thank the Fulbright Program for a Research Scholar Fellowship (A.V.) and Dr. Kristina Hamill for helping with the biological assays.

Keywords: cellular uptake · dendrimers · drug delivery · guanidinium-rich transporters · guanidinoglycosides · PAMAM

- [1] a) A. D. Frankel, C. O. Pabo, *Cell* **1988**, *55*, 1189–1193; b) M. Green, P. M. Loewenstein, *Cell* **1988**, *55*, 1179–1188.
- [2] a) P. A. Wender, W. C. Galliher, E. A. Goun, L. R. Jones, T. H. Pillow, *Adv. Drug Delivery Rev.* **2008**, *60*, 452–472; b) T. A. Theodossiou, A. Pantos, I. Tsogas, C. M. Paleos, *ChemMedChem* **2008**, *3*, 1635–1643; c) C. V. Bonduelle, E. R. Gillies, *Pharmaceuticals* **2010**, *3*, 636–666.
- [3] a) E. Geihe Stanzl, B. M. Trantow, J. R. Vargas, P. A. Wender, *Acc. Chem. Res.* **2013**, *46*, 2944–2954; b) D. M. Copolovici, K. Langel, E. Eriste, U. Langel, *ACS Nano* **2014**, *8*, 1972–1994; c) Q. Zhang, H. Gao, Q. He, *Mol. Pharm.* **2015**, *12*, 3105–3118.
- [4] Y. A. Fillon, J. P. Anderson, J. Chmielewski, *J. Am. Chem. Soc.* **2005**, *127*, 11798–11803.
- [5] a) M. Rueping, Y. Mahajan, M. Sauer, D. Seebach, *ChemBioChem* **2002**, *3*, 257–259; b) N. Umezawa, M. A. Gelman, M. Haigis, R. T. Raines, S. H. Gellman, *J. Am. Chem. Soc.* **2002**, *124*, 368–369.
- [6] P. A. Wender, D. J. Mitchell, K. Pattabiraman, E. T. Pelkey, L. Steinman, J. B. Rothbard, *Proc. Natl. Acad. Sci. USA* **2000**, *97*, 13003–13008.
- [7] P. A. Wender, J. B. Rothbard, T. C. Jessop, E. L. Kreider, B. L. Wylie, *J. Am. Chem. Soc.* **2002**, *124*, 13382–13383.

- [8] P. Zhou, M. Wang, L. Du, G. W. Fisher, A. Waggoner, D. H. Ly, *J. Am. Chem. Soc.* **2003**, *125*, 6878–6879.
- [9] C. J. McKinlay, R. M. Waymouth, P. A. Wender, *J. Am. Chem. Soc.* **2016**, *138*, 3510–3517.
- [10] a) E. Vives, *J. Controlled Release* **2005**, *109*, 77–85; b) Y. Huang, Y. Jiang, H. Wang, M. C. Shin, Y. Byun, H. He, Y. Liang, V. C. Yang, *Adv. Drug Delivery Rev.* **2013**, *65*, 1299–1315; c) N. Q. Shi, X. R. Qi, B. Xiang, Y. A. Zhang, *J. Controlled Release* **2014**, *194*, 53–70; d) E. Koren, V. P. Torchilin, *Trends Mol. Med.* **2012**, *18*, 385–393; e) J. Grunwald, T. Rejtar, R. R. Sawant, Z. Wang, V. P. Torchilin, *Bioconjugate Chem.* **2009**, *20*, 1531–1537; f) E. Koren, A. Apte, R. R. Sawant, J. Grunwald, V. P. Torchilin, *Drug Delivery* **2011**, *18*, 377–384.
- [11] E. Wexselblatt, J. D. Esko, Y. Tor, *J. Org. Chem.* **2014**, *79*, 6766–6774.
- [12] a) N. W. Luedtke, P. Carmichael, Y. Tor, *J. Am. Chem. Soc.* **2003**, *125*, 12374–12375; b) L. Elson-Schwab, O. B. Garner, M. Schuksz, B. E. Crawford, J. D. Esko, Y. Tor, *J. Biol. Chem.* **2007**, *282*, 13585–13591; c) A. V. Dix, L. Fischer, S. Sarrazin, C. P. Redgate, J. D. Esko, Y. Tor, *ChemBioChem* **2010**, *11*, 2302–2310; d) M. Inoue, W. Tong, J. D. Esko, Y. Tor, *ACS Chem. Biol.* **2013**, *8*, 1383–1388.
- [13] M. Inoue, E. Wexselblatt, J. D. Esko, Y. Tor, *ChemBioChem* **2014**, *15*, 676–680.
- [14] a) S. Svenson, A. S. Chauhan, *Nanomedicine* **2008**, *3*, 679–702; b) L. M. Kaminskas, V. M. McLeod, C. J. H. Porter, B. J. Boyd, *Mol. Pharm.* **2012**, *9*, 355–373; c) A.-M. Caminade, C.-O. Turrin, *J. Mater. Chem. B* **2014**, *2*, 4055–4066; d) Y. K. Katare, R. P. Daya, C. S. Gray, R. E. Luckham, J. Bhandari, A. S. Chauhan, R. K. Mishra, *Mol. Pharm.* **2015**, *12*, 3380–3388.
- [15] a) J. B. Rothbard, T. C. Jessop, P. A. Wender, *Adv. Drug Delivery Rev.* **2005**, *57*, 495–504; b) I. Tsogas, D. Tsiourvas, G. Nounesis, C. M. Paleos, *Langmuir* **2006**, *22*, 11322–11328; c) H. Maeda, L. W. Seymour, Y. Miyamoto, *Bioconjugate Chem.* **1992**, *3*, 351–362; d) H. Maeda, J. Wu, T. Sawa, Y. Matsumura, K. Hori, *J. Controlled Release* **2000**, *65*, 271–284.
- [16] a) J.-B. Kim, J. S. Choi, K. Nam, M. Lee, J.-S. Park, J.-K. Lee, *J. Controlled Release* **2006**, *114*, 110–117; b) H. Y. Nam, H. J. Hahn, K. Nam, W. Choi, Y. Jeong, D. Kim, J.-S. Park, *Int. J. Pharm.* **2008**, *363*, 199–205; c) T.-I. Kim, C. Z. Bai, K. Nam, J.-S. Park, *J. Controlled Release* **2009**, *136*, 132–139; d) X. Liu, C. Liu, J. Zhou, C. Chen, F. Qu, J. J. Rossi, P. Rocchi, L. Peng, *Nanoscale* **2015**, *7*, 3867–3875.
- [17] A. Ghilardi, D. Pezzoli, M. C. Bellucci, C. Malloggi, A. Negri, A. Sganappa, G. Tedeschi, G. Candiani, A. Volonterio, *Bioconjugate Chem.* **2013**, *24*, 1928–1936.
- [18] J. D. Esko, T. E. Stewart, W. H. Taylor, *Proc. Natl. Acad. Sci. USA* **1985**, *82*, 3197–3201.
- [19] E. Wexselblatt, J. D. Esko, Y. Tor, *ACS Nano* **2015**, *9*, 3961–3968.

Manuscript received: August 1, 2016

Accepted Article published: November 2, 2016

Final Article published: December 2, 2016